High-Performance Silicon Photonics Optical Filters with High-Order Distributed Feedback Resonators

Claudio Porzi[1], Graham J. Sharp[2], Marc Sorel[2], Antonella Bogoni[1]
[1] TeCIP Institute, Scuola Superiore Sant'Anna, 56124 Pisa - Italy
[2] School of Engineering, University of Glasgow, Glasgow, G12 8LP - United Kingdom
e-mail: c.porzi@santannapisa.it

ABSTRACT

Silicon photonics tunable passband optical filters with flat-top feature, large out-of-band rejection in excess of 40 dB, ultra-fast roll-off up to 1,000 dB/nm, and unprecedented passband-to-stopband ratio for high-index-contrast technology have been fabricated and characterized. The integrated filters are based on high-order distributed-feedback resonators implemented with cascaded phase-shifted Bragg gratings in silicon strip waveguides. Local micro-heaters are used for finely controlling the phases of the individual cavities of the coupled resonators and for providing additional tuning mechanism. Two different coupled-cavity resonators with passband widths of 25 GHz and 2 GHz, realized with 6th- and 5th- order filter designs, respectively, are exemplarily reported.

Keywords: Silicon photonics, integrated optical filters, waveguide Bragg gratings, Fabry-Perot filters.

1. INTRODUCTION

Integrated optical filters (OFs) boost the performances of photonic-integrated circuits (PICs), as they are required in almost any advanced operation dealing with handling and processing optical signals. In particular, the implementation of OFs through silicon-on-insulator (SOI) technological platform is highly sought after for the development and large-volume production of ultra-compact highly-functional PICs. To this scope, a huge amount of research has concentrated in the last decades on high-order coupled micro-ring resonators (MRRs), which proofed excellent performances for applications spanning from telecom/datacom to sensing and microwave photonics systems [1]-[3]. Few attention has been however devoted to integrated distributed Bragg resonators which, complimentary to the traveling-wave cavity of MRRs, implement standing-wave cavity resonators. Recently, we demonstrated high-order designs of such important class of OFs using phase-shifted Bragg gratings (PSBGs) realized in silicon strip waveguides [4]-[5]. In coupled SOI MRRs, the trade-off between ring dimensions and the ability of controlling small coupling coefficients for high-index-contrast waveguides makes challenging to realize OFs simultaneously exhibiting arbitrarily narrow passband widths and large free-spectral range (FSR) values. To date, maximum reported value of stopband-to-passband ratio in high-order silicon MRRs is about 100 [2]. On the other hand, PSBGs rely on an extremely short effective cavity of the order of the optical wavelength, which allows in principle for FSR-free operation. The range of wavelengths over which filtering operation is defined is set in this case by the grating stopband, which can be made relatively large using high-index-contrast silicon strip waveguides. To counteract the scattering of resonances among the coupled cavities in high-order filters due to unavoidable fabrication imperfections, local micro-heaters (MHs) have been successfully demonstrated for 3rd-order designs [5].

Here, we report the latest results relative to higher-order designs, enabling the realization of silicon photonics OFs with advanced features. A box-like 25 GHz-bandwidth passband transfer function with an out-of-band rejection larger than 45 dB within a 16-nm stopband region is realized in a 6th- order PSBGs, whereas a 5th- order design is exploited to realize a 2-GHz bandwidth filter with a roll-off of 1,000 dB/nm and a stopband-to-passband ratio larger than 600, confirming the unique potentials of this technique.

2. DEVICE SCHEMATIC AND FABRICATION

An integrated high-order distributed feedback resonator is obtained by cascading several symmetric waveguide Bragg Gratings (BGs) that, as in the proposed implementation schematized in Fig. 1(a), can be realized by periodically alternating two quarter-wave long waveguide sections with different width. Due to the BGs symmetry, half-wave cavities (HWCs) are formed at each interface between adjacent BG mirrors, supporting a resonant mode at the Bragg wavelength in the transmission spectrum with the typical Lorentzian shape. For M+1 BGs there are M coupled cavities, so that the overall filter transmission response can be constructed in a way much similar to coupled MRRs by controlling the Q-factor of the individual cavities through the lateral waveguide corrugation width ΔW and the number of periods N_i of the i^{th} BGs. Local MHs are placed above the HWCs cavities for correcting the slight deviations in the optical path from their nominal half-wave values at the Bragg wavelength. Additionally, the MHs offer a convenient mean for tuning the passband window while keeping the stopband edges fixed [5], thus improving the useful wavelength range of the filtering operation. Broader although rigid tuning can

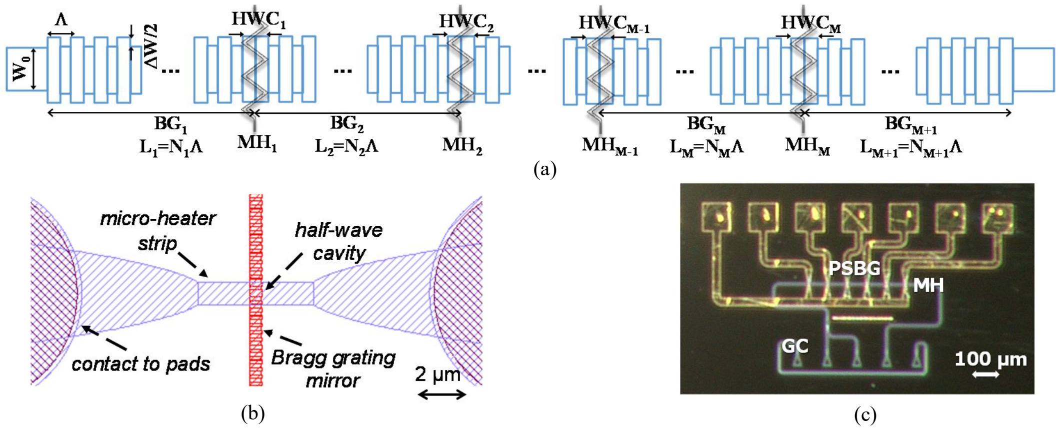

Figure 1. (a): High-order phase-shifted waveguide Bragg grating (PSBG) schematic structure; (b): Details of micro-heater (MH) mask layout; (c): Picture of a fabricated 6th-order device.

be accomplished by heating the whole grating structure [4]. The PSBGs were fabricated through electron-beam lithographic process on a silicon-on-insulator (SOI) wafer with a 3 µm-thick buried oxide layer and a 220 nm-thick core layer. The average grating waveguide width W_0 has been set to 500 nm, and the period of the corrugation Λ to 320 nm. Grating couplers (GCs) are used for vertical coupling with the input/output optical fibers. The MHs are formed by a 50 nm-thick, 1 µm-wide and 5 µm-long nichrome strip deposited on the top of a 1 µm-thick silica cladding layer. The MH mask layout is shown in Fig. 1(b). Gold metal lines and pads are used for connecting the MHs to current sources through contact probes. The typical measured contact resistance of the MHs is ~350 Ω. An image of a fabricated sample, corresponding to a 450 µm-long 6th-order PSBG design, is shown in Fig. 1(c).

3. DEVICES CHARACTERIZATION

The first considered device corresponds to a 6th-order (M=6) design with a nominal lateral waveguide corrugation ΔW of 60 nm. The measured spectral transmission, normalized to GC response, without and with cavity tuning is reported in Figure 2(a). After applying proper control signals to each MH, a sharp transmission window exhibiting an out-of-band rejection in excess of 45 dB over a 16 nm-wide stopband region is observed. The insertion loss at peak transmission is ~2.8 dB. Numerical fitting of the tuned response using the design parameters reported in the figure caption is also shown. The details of the passband window are also shown in Fig. 2(b), illustrating the flat-top box-shaped feature of the filter transfer function, with a measured maximum ripple of 0.1 dB within the 18.5 GHz-wide -1dB bandwidth. The -3dB and -40 dB bandwidth values are 24 GHz and 45.8 GHz, respectively, for a corresponding transition band roll-off of more than 400 dB/nm (3.4 dB/GHz). Finally, the passband-to-stopband ratio is ~75.

In the second considered design, targeting a narrower filter bandwidth, a higher loaded Q-factor for the HWCs is investigated. In order to mitigate the larger sensitivity to propagation loss as energy is stored for longer time within the resonator, both the filter order and grating coupling coefficient are reduced. In particular, a 5th-order (M=5) distributed feedback resonator has been constructed by cascading six waveguide BG mirrors using a nominal width variation ΔW of 48 nm. The results of device characterization are summarized in Figure 3. Also for

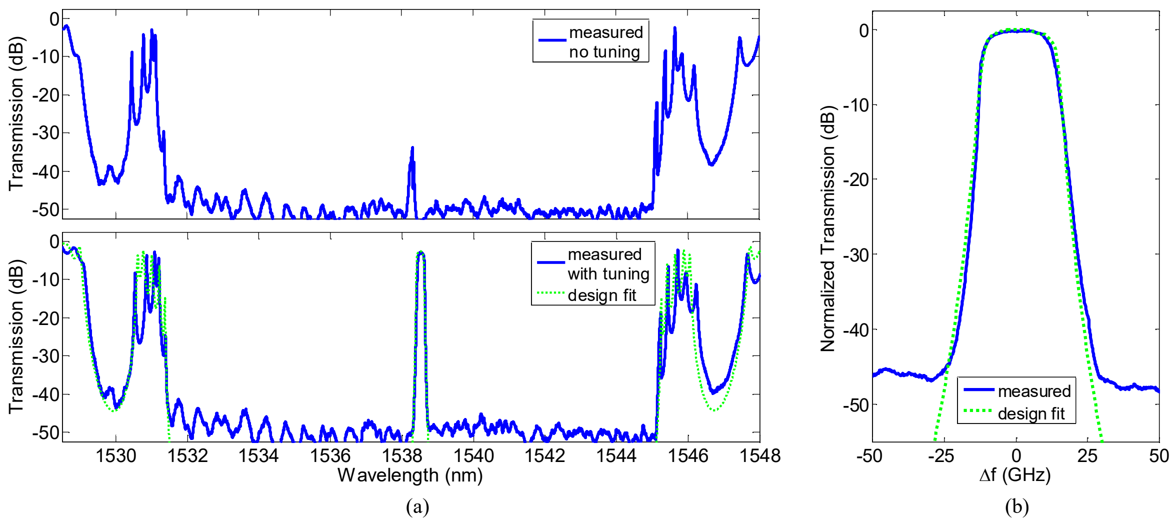

Figure 2. (a): Spectral transmission of 6th-oreder PSBG without and with control signals to MHs; Design period numbers for the Bragg grating mirrors: N_1=N_6=112; N_2=N_5=224; N_3=N_4=234; N_6=236; (b): Details of passband window.

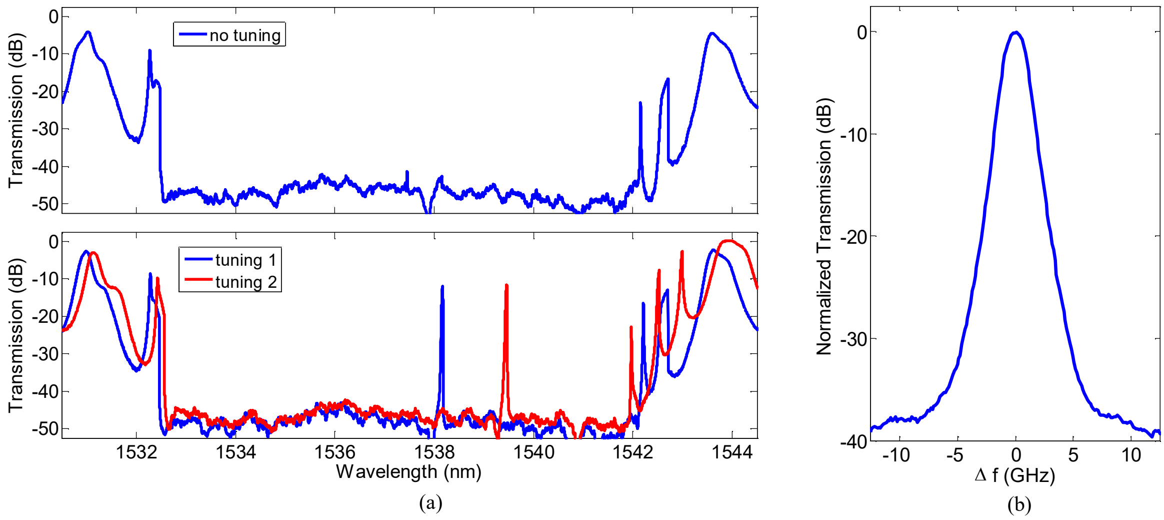

Figure 3. (a): Spectral transmission of 5th-oreder PSBG without and with control signals to MHs; (b): Details of passband window.

this case, a tuning of the resonances by individually heating each QWCs through the MHs is used to optimize the passband response to nearly 40 dB out-of-band rejection, as illustrated in Fig. 3(a). Two different levels of tuning settings are shown, from which it can be seen that heating the HWCs only slightly affect the spectral location of the stopband edges. The corresponding absorbed power excursion for the considered passband shift of ~1.3 nm is less than 2 mW for each MHs. By reducing the optical path of the HWCs from their nominal value, resonance tuning from the shorter-wavelength stopband edge side toward the longer-wavelength one can be realized. As an effect of the reduced corrugation depth for this structure, the stopband width is now ~9.5 nm. However, due to the stronger loaded Q-factor provided by proper period numbers in the BG mirrors, a very narrow and steep passband window is observed, as illustrated in Fig. 3(b). The measured -1dB and -3dB bandwidth values are 1.2 GHz and 2 GHz, respectively, for a remarkably large stopband-to-passband ratio of more than 600. As expected, the stronger sensitivity to propagation loss in this case rounds the passband window top and raises the insertion loss to ~10 dB. The effect of propagation loss in such high Q-factor structures could be reduced by using a for instance sinusoidal or triangular corrugation patterns rather than the rectangular one for the waveguide grating. Nevertheless, the sharpness of the filter transfer function is fairly preserved, with a measured -33 dB bandwidth of 9.4 GHz, for a roll-off as large as 8 dB/GHz (1,000 dB/nm) in a 3.7 GHz-wide transition bandwidth spanning over 30 dB.

4. CONCLUSIONS

We reported on the fabrication and characterization of advanced silicon photonics optical filters based on high-order phase-shifted waveguide Bragg gratings encompassing local micro-heaters for finely controlling and tuning the filter response. Design flexibility is highlighted by considering two different design concepts; a 24 GHz-bandwidth passband transfer function exhibiting box-like features with an out-of-band rejection in excess of 45 dB and 1.75 THz-wide stopband region is observed for a 6th-order cavity, whereas a high Q-factor 5th-order design provided an ultra-narrow filter bandwidth of 2 GHz, extremely fast roll-off, and stopband-to-passband ratio of 600.

ACKNOWLEDGEMENTS

The authors acknowledge the support from the technical staff at the James Watt Nanofabrication Centre (JWNC) at Glasgow University. The work was partially funded by the Engineering and Physical Sciences Research Council (EPSRC) under the CORNERSTONE project (EP/L021129/1), and by the Italian National projects PHOOD and PREVENTION.

REFERENCES

[1] M. A. Popovic, *et al.*: Tunable, fourth-order silicon microring-resonator add-drop filters, *in Proc. ECOC 2007*, Berlin, Germany, Sept. 2007, paper 1.2.3.

[2] P. Dong, et al.: GHz-bandwidth optical filters based on high-order silicon ring resonators, Opt. Express, vol. 18, pp. 23784-23789, Nov. 2010.

[3] W. Bogaerts, *et al.*: Silicon microring resonators, *Laser & Photonics Reviews*, vol. 6, pp. 47-73, Jan. 2012.

[4] C. Porzi, *et al.*: Integrated Passband Optical Filter with High-Order Phase-Shifted Bragg Grating in Silicon-on-Insulator Technology, *in Proc. ECIO 2018*, Valencia, Spain, May-June 2018, paper Fr.1.B.4.

[5] C. Porzi, *et al.*: High-Contrast, Flat-Top, Silicon-Photonics Passband Optical Filters with High-Order Phase-Shifted Bragg Gratings, *in Proc. ECOC 2018*, Roma, Italy, Sep. 2018, paper Mo3C.5.